51. IWK
Internationales Wissenschaftliches Kolloquium
International Scientific Colloquium

PROCEEDINGS

11-15 September 2006

FACULTY OF ELECTRICAL ENGINEERING AND INFORMATION SCIENCE

INFORMATION TECHNOLOGY AND ELECTRICAL ENGINEERING - DEVICES AND SYSTEMS, MATERIALS AND TECHNOLOGIES FOR THE FUTURE

Startseite / Index:
http://www.db-thueringen.de/servlets/DocumentServlet?id=12391

TECHNISCHE UNIVERSITÄT ILMENAU

Impressum

Herausgeber: Der Rektor der Technischen Universität Ilmenau
Univ.-Prof. Dr. rer. nat. habil. Peter Scharff

Redaktion: Referat Marketing und Studentische Angelegenheiten
Andrea Schneider

Fakultät für Elektrotechnik und Informationstechnik
Susanne Jakob
Dipl.-Ing. Helge Drumm

Redaktionsschluss: 07. Juli 2006

Technische Realisierung (CD-Rom-Ausgabe):
Institut für Medientechnik an der TU Ilmenau
Dipl.-Ing. Christian Weigel
Dipl.-Ing. Marco Albrecht
Dipl.-Ing. Helge Drumm

Technische Realisierung (Online-Ausgabe):
Universitätsbibliothek Ilmenau
ilmedia
Postfach 10 05 65
98684 Ilmenau

Verlag:
Verlag ISLE, Betriebsstätte des ISLE e.V.
Werner-von-Siemens-Str. 16
98693 Ilrnenau

© Technische Universität Ilmenau (Thür.) 2006

Diese Publikationen und alle in ihr enthaltenen Beiträge und Abbildungen sind urheberrechtlich geschützt. Mit Ausnahme der gesetzlich zugelassenen Fälle ist eine Verwertung ohne Einwilligung der Redaktion strafbar.

ISBN (Druckausgabe): 3-938843-15-2
ISBN (CD-Rom-Ausgabe): 3-938843-16-0

Startseite / Index:
http://www.db-thueringen.de/servlets/DocumentServlet?id=12391

51st Internationales Wissenschaftliches Kolloquium
Technische Universität Ilmenau
September 11 – 15, 2006

V. Kireev / R. Volkert / E. Kallenbach / N. Gorbatenko

Hysteresis Compensation for Electromagnetic Actuators Applied in a Planar Magnetic Guidance System

Introduction

By combining electrodynamic planar actuators with magnetic guidance elements, reliable high-precision vacuum-compatible integrated multi-coordinate positioning systems can be designed, which are required for many modern applications, e.g. for the manufacture of integrated circuits. Compared to the well-known multi-coordinate drives with aerostatic bearings, no disturbance forces due to air supply pipes to the moving platform, no wear of these supply pipes as well as no guidance oscillations through variations of the supply pressure can occur in a magnetically guided system. Furthermore, active magnetic guidances allow an extended functionality: By means of a suitable control system as well as an appropriate configuration of the guidance actuators movements in six degrees of freedom with a single movable element and hence with high dynamics can be realized. An operation of the drive in vacuum and in clean rooms is possible.

1. Structure and operation principle of the actuator

The actuator shown in Fig. 1 can serve as a single guidance element for micro- and nano-positioning stages with relatively large planar strokes [1]. Using several actuators, a complete multi-coordinate drive can be built up.

In a certain vertical position of the moving part (slider) an unstable equilibrium of forces generated by the flux of four permanent magnets occurs. A stable levitation of the moving part can only be achieved through an active control of the current in the coils. Thus, the magnetic flux can be increased in one air gap and at the same time decreased in the other air gap. The maximal guidance force of such an actuator is 60…270 N and depends on the z-position of the slider.

For propulsion of the movable element in x-direction the stator elements must be wound with additional coils (not shown in Fig. 1). The propulsion forces due to these coils are relatively low (8…10 N).

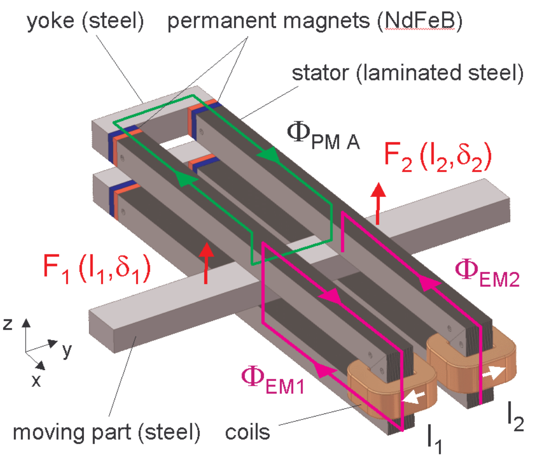

Fig. 1: Operation principle of an actuator element [1]

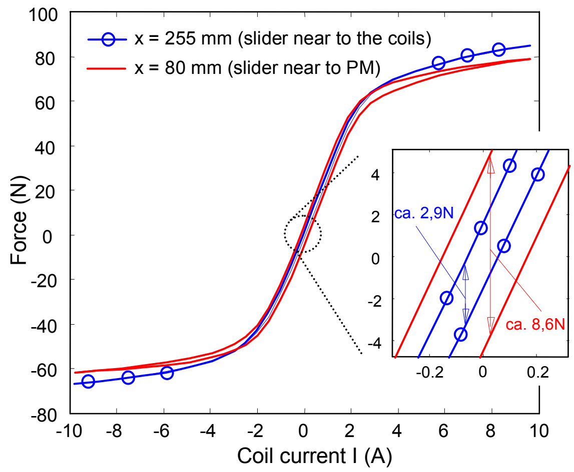

Fig. 2: Force hysteresis depending on the horizontal slider position

The actuator is characterized by a variable z-force hysteresis. The width of the hysteresis loop and the maximum force value depend on the moving part's horizontal (x) and vertical (z) position and consequently on the volume of magnetic material, which has to be demagnetized by a variable coil current (Fig. 2). To attain a linear force-current relation, the non-linearity and the hysteresis have to be compensated in real-time.

Among some other variants, the model developed by D.C. Jiles and D.L. Atherton Jiles-Atherton has been chosen for the modeling of ferromagnetism in soft magnetic materials, such as electrical steel, and for the force hysteresis.

2. The Jiles-Atherton-Model

The Jiles-Atherton model is a statistical mechanical model. Although it was developed over the course of several publications, the classic paper is generally considered to be [2]. D. Jiles later published an entire text on magnetics, which contains the model, as well as extensions such as stress effects [3]. The model takes into account the actual physical processes inside a magnetic material. Movement and adhesion of magnetic domain borders near crystal defects cause a reversible magnetisation. An irreversible magnetisation arises from deformations of the domain borders. These effects are realised as variations from the anhysteretic curve. The Jiles-Atherton model offers a high accuracy and was mainly recommended for FEM calculations [4]. Originally it is based on the Langevin model to calculate the magnetisation of paramagnetic materials. Langevin developed the relation between field strength H and magnetisation M with:

$$M = M_S \cdot \left(\coth\left(\frac{H}{a} \right) - \frac{a}{H} \right). \tag{1}$$

Thereby the parameter a is a material constant. The factor M_S (saturation magnetisation) arises for $H \to \infty$ and leads theoretically to a parallel orientation of all magnetic moments and to the applied field strength. For ferromagnetic materials Weiß introduced the "effective field" H_e. It is caused by the interaction of single domains, which generate an independent field $\overline{\alpha} \cdot M$, similar to a permanent magnet, due to the applied field strength and irreversible processes. The applied field strength and the independent field $\overline{\alpha} \cdot M$ result in the effective field strength:

$$H_e = H + \overline{\alpha} \cdot M\,. \tag{2}$$

The factor $\overline{\alpha}$ represents a magnetic field parameter for the quantitative description of domain interactions. Eq. (1) can be reshaped to calculate the anhysteretic magnetisation M_{an} for ferromagnetic materials:

$$M_{an} = M_S \cdot \left(\coth\left(\frac{H_e}{a} \right) - \frac{a}{H_e} \right), \tag{3}$$

$$M_{an} = M_S \cdot \left(\coth\left(\frac{H + \overline{\alpha} \cdot M}{a} \right) - \frac{a}{H + \overline{\alpha} \cdot M} \right). \tag{4}$$

To model the hysteresis of a material, Jiles and Atherton use a reversible part M_{rev} and an irreversible part M_{irr} for the magnetisation:

$$M = M_{rev} + M_{irr}\,. \tag{5}$$

For the irreversible part M_{irr} applies:

$$\frac{\mathrm{d}\,M_{irr}}{\mathrm{d}\,H} = \frac{M_{an}(H_e) - M_{irr}}{k \cdot \mathrm{sgn}\left(\frac{\mathrm{d}\,H}{\mathrm{d}\,t} \right) - \overline{\alpha} \cdot (M_{an}(H_e) - M_{irr})}\,. \tag{6}$$

The constant k is a degree for the energy losses per volume unit due to the resulting field M. By integration the irreversible component yields:

$$M_{irr} = \int \frac{\mathrm{d}\,M_{irr}}{\mathrm{d}\,H}\,\mathrm{d}\,H \,. \tag{7}$$

For the magnetisation *M* follows:

$$M = (1 - c) \cdot M_{irr} + c \cdot M_{an}(H_e) \tag{8}$$

with the reversibility coefficient *c*. From magnetisation *M* and field strength *H* the magnetic induction *B* is calculated:

$$B = \mu_0 \cdot (H + M)\,. \tag{9}$$

The magnetic *B-H* hysteresis is the reason for the force-current (*F-I*) hysteresis of electromagnets. Though, because of stray fields and inhomogeneities at the working air gap, the hystereses cannot be converted into each other. By means of a coordinate transformation (shifting, scaling) the *F-I* hysteresis can be mapped onto the point of origin. Then it acquires a shape similar to the one of the *B-H* hysteresis. The following experimentally gained transformation equations were applied:

$$H = c_H \cdot I \tag{10}$$

$$F = c_B \cdot B^2 \tag{11}$$

Due to the transformation, the *F-I* hysteresis is mapped onto the *B-H* hysteresis model. Therefore the five Jiles-Atherton model parameters a, M_S, $\overline{\alpha}$, k and c become abstract values, which cannot be assigned to certain characteristics of the *F-I* hysteresis loop. Yet to simplify matters, the original denotations were retained, although it is formally incorrect.

2.1 Identification of the model parameters

Exemplarily the *F-I* hysteresis loops of an electromagnet, which was designed as part of a magnetic guidance system, were measured for several air gap lengths δ_i (reference points) and currents. The applicability of the Jiles-Atherton model to describe the *F-I* hysteresis has to be proven. Therefore search algorithms are used to find suitable parameter sets for the five model parameters a, M_S, $\overline{\alpha}$, k, c and the two introduced scaling parameters c_H and c_B, which allow an exact reproduction of the measured hysteresis loops. This task can be converted into an optimisation problem with seven parameters (Fig. 3).

To define the quality of a parameter set, the sum of deviations between calculated and measured hysteresis curve at certain measuring points is determined (eq. 12). The optimisation algorithm tries to minimise this quality criterion.

$$Q_{JA} = \min\left[\sum_{j=1}^{j_{mp}} \left|F_{calc,j} - F_{meas,j}\right|\right], \qquad (12)$$

where j_{mp} denotes the number of measuring points.

For higher accuracies also inner hysteresis loops are included in the parameter identification.

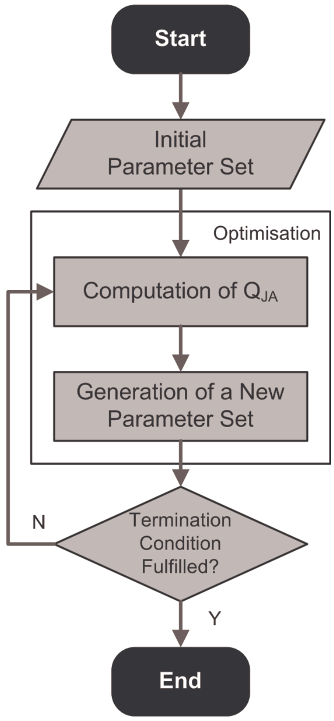

Fig. 3: Optimisation procedure.

2.2 Optimisation algorithms

Ströhla and Bode [5] investigated some optimisation algorithms with regard to their applicability for this task. The possible solution space is first narrowed by an evolutionary optimisation algorithm according to Schwefel [6] in a very efficient way. Then for a more exact optimum localisation the well-known Nelder-Mead Simplex algorithm is executed starting with the parameter set found by the evolutionary search procedure.

Thus for every reference air gap an optimal parameter set was computed. In Fig. 4 the values found for the parameters k and c_H are marked with circles. Between these points spline interpolations were applied.

With the obtained parameter sets the measured F-I hystereses can be reproduced at the reference points in a highly accurate way. Yet, a parameter interpolation for air gap lengths between the measured reference points does not lead to physically reasonable results. The hysteresis loops calculated with interpolated parameters do not run between the loops evaluated for the adjoining reference points, but rather incoherent. Other optimisations with seven variable parameters show similar results.

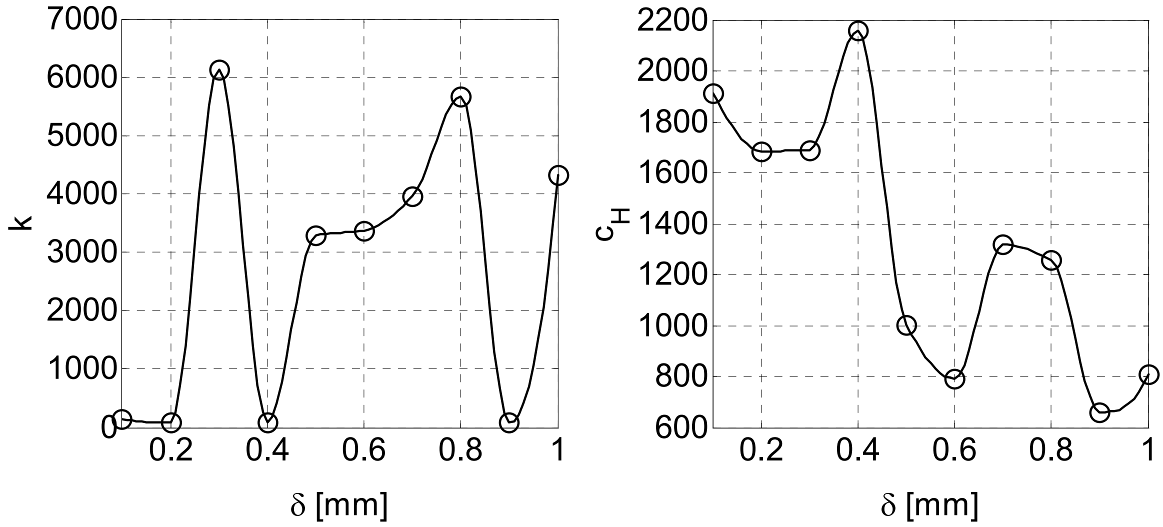

Fig. 4: Spline interpolated curves for the model parameters k and c_H, gained from optimisations.

2.3 Reduction of the number of variable parameters

Therefore, for a real-time application the parameter optimisation procedure was modified to enable a realistic reproduction of the F-I hysteresis for every possible air gap length within the working range of the electromagnet. Thereby it was aspired, to keep constant as many parameters as possible, i.e., to reduce the number of variable parameters, which are necessary to calculate the hysteresis loops for different air gap lengths.

A procedure with several optimisation cycles, where the number of free parameters necessary to calculate the hysteresis loops for different air gap lengths is reduced step by step and the remaining parameters are kept constant, was successfully investigated (Fig. 5). The best result was gained with c_H as the only free parameter. For $c_H(\delta)$ (dependency of c_H on the air gap length) a continuous, almost quadratic curve arises.

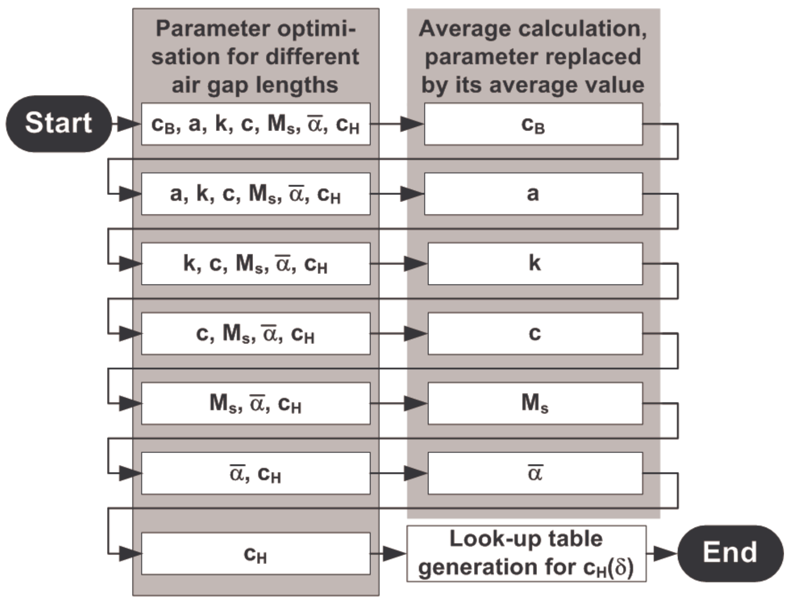

Fig. 5: Parameter optimisation sequence.

The best results were gained with c_H as the only variable parameter. For $c_H(\delta)$ (dependency of c_H on the air gap length δ) a continuous curve arises (Fig. 6).

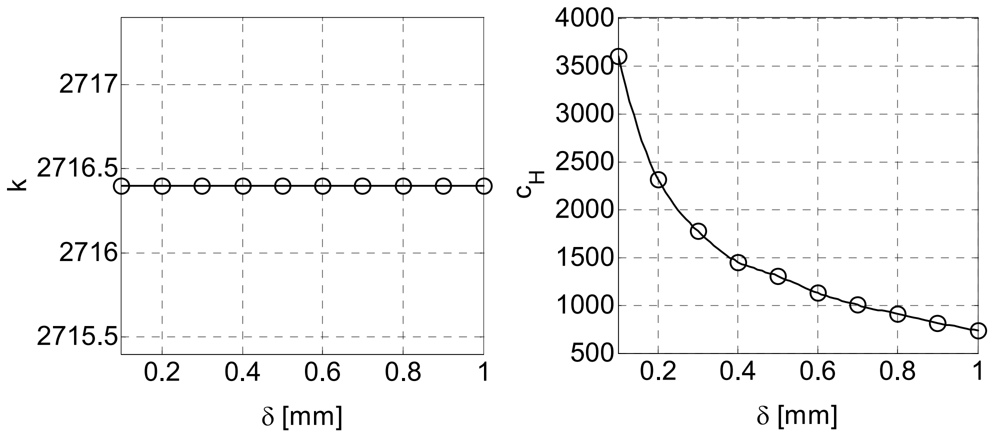

Fig. 6. Curves for the parameters *k* and c_H, gained from the modified optimisation sequence.

The usage of c_H as the only variable parameter implicates the advantage, that the Jiles-Atherton model can be computed with the same inner model parameters for all air gap lengths. Subsequently the result is scaled through a multiplication by c_H (eq. 10).

To verify the results, again hysteresis loops for air gaps between the reference points were calculated. Now these hysteresis loops run exactly between those for the adjoining reference points, as shown Fig. 7. Thus the applicability of the identification procedure for the parameter of the *F-I* hysteresis model was proven.

To determine the Jiles-Atherton model parameters, at first the force-current hysteresis curves for different air gaps and x-positions have to be measured once.

A search algorithm has to be applied to minimize the deviation between measured and modelled hysteresis curve. In recent experiments close compliances were gained with a combination of the evolutionary search algorithm according to Schwefel and the Nelder-Mead simplex method.

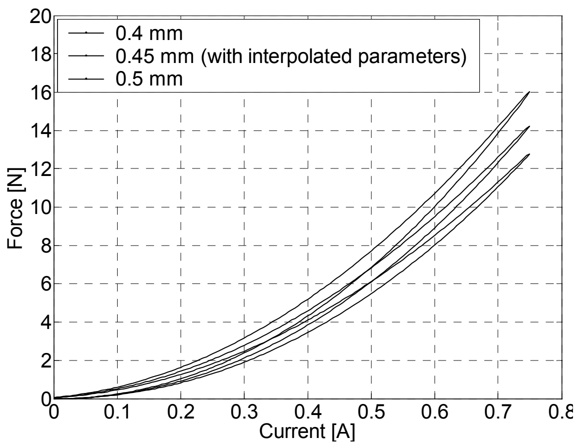

Fig. 7: Calculated hysteresis curves for different air gaps. The curve for δ = 0.45 mm is correct.

3 Position Controller with Hysteresis Compensation

By using the inverse Jiles-Atherton model as part of the controller, the electromagnet's force-current hysteresis is compensated and therefore a linear actuator characteristic can be achieved. Based on simulation results, a PID controller with an additional derivative part (PIDD2-controller) in combination with the inverse Jiles-Atherton model was applied and several step responses with different heights were measured. Alternatively a PIDD2 controller without hysteresis compensation was investigated. With hysteresis compensation an overshoot reduction by 50% was gained. The settling time and steady state error remain almost constant.

Exemplarily a position controller with hysteresis compensation was tested in a real-time hardware-in-the-loop test rig with a single electromagnet, which was originally developed as part of a magnetic guidance system. Fig. 8 shows typical results.

The most promising results have been achieved by the compensation of the non-linearity of the actuator for the average F-I characteristic.

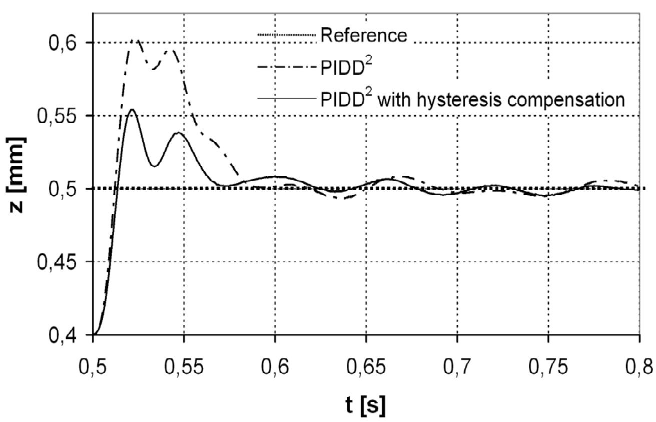

Fig. 8: Effect of the hysteresis compensation

Since the hysteresis compensation is a very time consuming and computational intensive task, the use of FPGA can be a good supplement to an ordinary DSP solution [7].

Conclusion

A single planar magnetic guidance element was presented. Three or four of those actuator units may be used to build up a complete multi-coordinate drive, which offers a relatively large planar movement range. Measurements at a single actuator element revealed a magnetic hysteresis depending on the horizontal and vertical position of the slider. For a position controller this effect acts as a disturbing influence limiting the control performance.

To compensate the force-current hysteresis measured at the guidance system, an inverse Jiles-Atherton hysteresis model were applied. Experiments with a position controller for a test electromagnet revealed an improved control performance arising from the real-time non-linearity and hysteresis compensation.

References:

[1] Overschie, P.M., L. Jabben, J. van Eijk and A. Molenaar (2001). Design of a 6-DoF Contactless Motion Stage with Stationary Magnets and Coils. In: Proceedings of the 6th International Symposium on Magnetic Suspension Technology, Politecnico di Torino, Italy, pp. 157-162.

[2] Jiles, D.C. and D.L. Atherton (1986). Theory of Ferromagnetic Hysteresis. In: Journal of Magnetism and Magnetic Materials, vol. 61, no. 1/2, pp. 48-60.

[3] Jiles, David Introduction to Magnetism and Magnetic Materials. Chapman & Hall, 1991.

[4] N. Sadowski, N.J. Batistela, J.P. Bastos, M. Lajoie-Mazenc: An Inverse Jiles-Atherton Model to Take into Account Hysteresis in Time-Stepping Finite-Element Calculations. IEEE Trans. Magn., vol. 38, no. 2, pp. 797–800, 2002.

[5] Ströhla, T. and S. Bode (2004). Compensation of the Force Hysteresis of Proportional Solenoid Actuators. In: Proceedings of the International IEEE Conference Mechatronics & Robotics, vol. 2, Aachen, Germany, pp. 442-445.

[6] Schwefel, H.P. 1977. Numerische Optimierung von Computermodellen mittels der Evolutions-strategien. Birkhäuser, Basel, Stuttgart.

[7] H. Janocha, D. Pesotski, K. Kuhnen. FPGA-Based Compensator of Hysteretic Actuator Nonlinearities for Highly Dynamic Applications. ACTUATOR 2006, 10th International Conference on New Actuators, 14-16.06.2006: Proceedings, p. 1013.

Authors:

Dipl.-Ing. V. Kireev, Dipl.-Ing. R. Volkert
Prof. Dr.-Ing. habil. E. Kallenbach
Technische Universität Ilmenau, FG Mechatronik
PF 10 05 65, D-98684 Ilmenau
Tel.: +49 3677 69 39 27
Fax: +49 3677 69 18 01
E-mail: vladimir.kireev@tu-ilmenau.de

Prof. dr. sc. tech Nikolaj Gorbatenko
South-Russia State Technical University
Prosveshenija 132,
346428 Novotcherkassk, Russia
Phone: +7 86352 55449
Fax: +7 86352 42056
E-mail: oms@novoch.ru